STRESS LINEARIZATION APPLICATION OF OBLIQUE NOZZLES WITH WELDED PAD REINFORCEMENT IN CYLINDRICAL PRESSURE VESSELS

Murat Bozkurt[1] , and David Nash[2]

[1]Department of Mechanical Engineering, Istanbul University - Cerrahpaşa

[2]Department of Mechanical and Aerospace Engineering, University of Strathclyde

Corresponding author(s):

Murat Bozkurt, Department of Mechanical Engineering, Istanbul University – Cerrahpaşa
Email: murat.bozkurt@iuc.edu.tr

ABSTRACT

In pressure vessel applications, one of the most feasible and economical ways of reinforcing an isolated nozzle is to use a pad or compensating plate. Where a pad is used, the extra material is considered to as effective as provided by a thick vessel plate, so a good fit in the vessel shell is required. Considering this information, in this study, welded pad reinforcement is applied to the oblique nozzle - cylinder intersections in the cylindrical pressure vessels and membrane stress and total stress (membrane + bending) cases are examined. It is well-known that the maximum stress is at the crotch corner (nozzle-cylinder junction) in the vertical junction of the radial nozzle. However, as the nozzle connection angle increases, the direction and magnitude of the stress should be investigated. For this reason, 6 critical paths were determined for the nozzle-cylinder junction and the stress distributions along these paths were examined with the help of Stress Linearization Analysis. In the analysis, cases such as oblique nozzle angle, pad reinforcement rates according to shell thickness, effect of increase in pad diameter are examined in detail. In conclusion, this study provides researchers with an alternative stress analysis for critical locations in the intersection area in the design and analysis of cylinder-oblique nozzle connections.

Keywords: Cylindrical Vessels, Nozzle, Pad Analysis, Stress Linearization

Notation

d_i: nozzle inner diameter

d_o: nozzle outer diameter

d_m: nozzle mean diameter

D_i: shell inner diameter

D_o: shell outer diameter

D_m: shell mean diameter

FEA: Finite Element Analysis

FEM: Finite Element Modelling

SLA: Stress Linearization Analysis

t: nozzle thickness

T: shell thickness

Tp: pad thickness

σ_m: membrane stress

Ψ: oblique nozzle connection angle

1. INTRODUCTION

In terms of engineering applications, structures such as pressure vessels, piping installations and reactors must be economical in terms of design criteria and, also high security. Especially for nozzle-shell junctions exposed to internal pressure and external loads, high stresses in the connection area should be reduced as much as possible. Therefore, in pressure vessel applications, one of the most convenient and economical ways to retrofit an insulated nozzle is to use a reinforcing pad or balancing plate. There are many studies in the literature for determination of critical stress regions and calculations. WRC107[1] and WRC537[2] are among the most widely used sources for calculating local stresses in pressure vessels.

Mukhtar and Gahtani carried out some studies for nozzle-cylinder intersections [3,4,5,6]. In summary, in these studies, stress concentration factors based on thin shell theory are obtained. These values are obtained separately for both the vessel and the nozzle and compared with the results in the literature. In another work, the results were enriched with tables of cylindrical containers intersecting with small diameter nozzles. Bozkurt et al. [7,8,9] conducted studies on nozzle combinations in cylindrical pressure vessels without any pad reinforcement. In these studies, a high-fidelity FE model has been developed in order to obtain more accurate results with the finite element method of the maximum stresses occurring in the crotch corners. Elastic and Elastic-Perfectly Plastic analysis (Limit Load Analysis) for various internal and external loads applied to the model were completed and the results were verified by comparing with WRC537

Cheema et al. [10] made finite element solutions for pad reinforced nozzles and compared the results with WRC107[1] and WRC297[11]. The authors stated that a forementioned bulletins could not respond to the geometrical limitations occurring in containers with large openings, and they introduced a comparison method with their study using FEM.

In pad applications around the nozzle, the shape of the pad and the rate of material contribution is also very important. In their study, Kharat et al. [12] compared the stress results they obtained with 4 different pad applications with FEA. In the light of the obtained results, the authors suggested 2 pad types were more suitable for the design procedure. Xue et al. [13] run a study for cylinder-nozzle intersections with and without reinforcement plates. The aim of the study was to determine the experimental limit pressure for a constant d/D parameter. With their test results, the authors noted that pad reinforcement significantly backed the container for the limit pressures. In a manner similar to a previous study, the strength behaviour of the structure for pad-reinforced and non-pad cylinder-cylinder intersections was investigated by Fang et al. [14]. Vessels were produced with different diameter ratios (d/D) for this study and obtained FEA results were supported the with these experiments. By determining the plastic limit moment load affecting the nozzle, load-strain curves were obtained for each test. The study provided a broad perspective for understanding pad usefulness on the pressure vessels and nozzle junctions. In addition, the authors have also focused on pad reinforced nozzles placed on Ellipsoidal pressure vessel heads. In 1986, Chao et al. [15] tried to understand the effects of the size and thickness of the nozzles located in the ellipsoidal pressure vessel head on radial flexibility using shell theory. In 1999, a study was carried out to determine the optimum pad sizes for the nozzle connections in the ellipsoidal pressure vessel heads by Nash et al. [16]. Moreover, design curves are presented for the allowable stress calculations of each applied forces. In 2002, Skopinsky et al. [17] was figured out stress analysis on pad-applied nozzles in

different configurations on the ellipsoidal heads of pressure vessels. The geometric parameters of the connections were discussed with the numerical and experimental results.

An important configuration is that of oblique nozzles for nozzle combinations in pressure vessels. As the angle between the nozzle and the shell changes, the maximum stress magnitudes also change. For this reason, the literature reports some significant studies on this subject as well. Petrovic et al. [18] completed a study on the moment effect caused by external loading on the oblique nozzle. The stress results were obtained with FEA are classified according to the maximum stress criteria. Weiß et al. [19] managed a comprehensive strength analysis for oblique nozzles in cylindrical pressure vessels. The fatigue behaviour of the nozzles was investigated in order to determine possible fatigue failure locations in nozzle connections subjected to internal pressure and axial loads. Additionally, Patel et al. [20] performed limit load analysis for multiple oblique nozzle connections. Finally, Robinson et al. [21] experimentally investigated the behaviour of oblique flush nozzles in spherical pressure vessels in the plastic region.

Based on all these results, it can be concluded that in nozzle connection problems, nozzle-cylinder connection areas form the weakest link of the chain and high stress concentrations occur in these opening areas. One of the most practical ways to manage the high stresses that may occur here is to provide pad reinforcements around the opening area. In this study, besides vertical nozzles, oblique connections placed at a certain angle with shell are examined In summary, the study investigates the effect of pad reinforcement on problems with nozzles placed vertically or at a certain angle in a cylindrical container. In line with this objective, critical paths are determined on the system after the limit loading analysis and stress linearization along these paths are calculated using a finite element approach. In this way, the maximum stress distributions at critical points are linearized and stress trends are displayed graphically on the determined critical paths.

2. FINITE ELEMENT MODELLING

In this section, the nozzle-cylinder connection is modelled using the ANSYS program [22]. The main variable in the model is the oblique nozzle connection angle (Ψ), and pad thickness. In accordance with the ASME BPV Code, Section VIII, Appendix l-7(b)l(b), the rules for "radial nozzles," not oblique or tangential, must meet strength requirements while building finite element models in pressure vessels. According to these rules, 3.4 (Rt)0.5 are greater than 40in. In that formula, D is the ratio of vessel diameter, and t is the shell thickness. For nozzles that exceed these parameters, a finite element analysis (FEA) should be performed [24]. Here, there is no standard procedure related to the mesh structure and boundary conditions to be applied while FE modelling is performed. For this reason, an open-ended pressure vessel, which is seated on 2 saddles and limited to movement from these saddles, was used while selecting the problem (see **Figure 1**). Here, there is no contact set between the saddle and the main vessel, and they are attached to each other through contacting keypoints. The mentioned situation is also valid for the combination of pad and vessel. Only the internal pressure load will be examined in the system. According to the applied internal pressure values, critical stress locations will be examined through the determined paths. Shell93 and Solid180 elements are used to obtain the most suitable mesh structure for the calculation of maximum stresses. The most appropriate mesh structure is obtained with the applied sweep mesh and mapping around the nozzle.

2.1. Selection of the Geometry and Materials

For finite element modelling, 3 different materials were used as can be seen in the **Figure 1**. SA-516 Grade 70 Carbon steel pressure vessel plate with a Young's modulus value of 200GPa was chosen for the shell material. For the nozzle material, ASTM A266 Grade 2 Carbon Steel, which has a Young's modulus value of 190GPa, was used. Since the saddles are not in the critical region to be examined, no specific material selection has been made and the Young's modulus was defined as 290GPa.

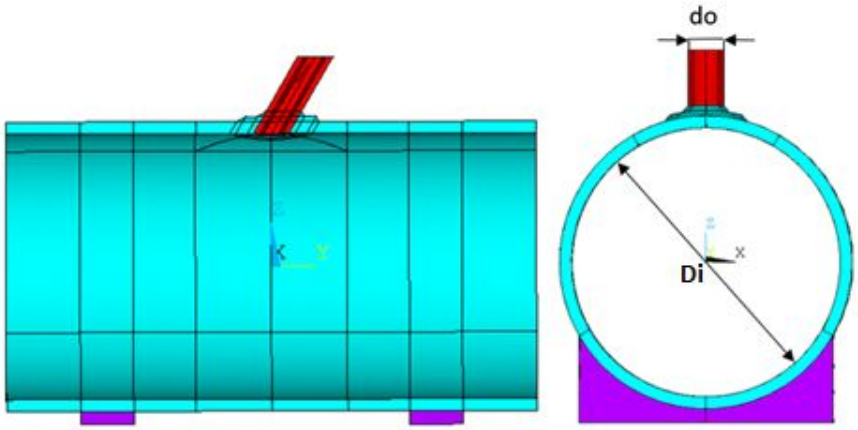

Figure 1. Cylindrical shell with a nozzle not radially arranged (oblique)

In these analyses, the nozzle inner diameter is always one quarter of the shell inner diameter. The system is only subject to internal pressure loading. From the saddle subfields, the model has fixed supported. It is noted that the shell is free to move from both ends. For cylindrical nozzles lying in a plane, higher stresses may occur in the lateral cross section. For this reason, the oblique nozzle angle (Ψ) should not exceed 50^0 [23]. In the light of this information, analysis will be performed such that the angle (Ψ) between the nozzle and the cylindrical container will be maximum 45^0. A representative representation of the oblique nozzle angle is given in the **Figure 2**.

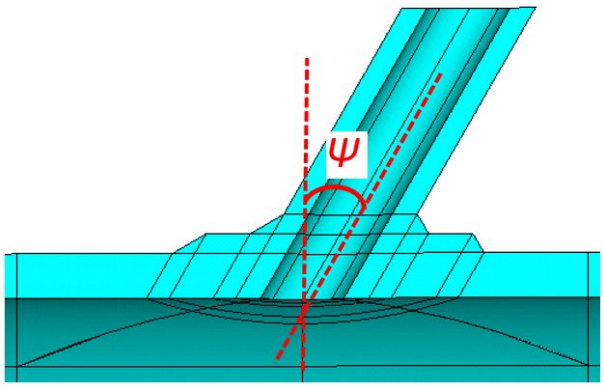

Figure 2. Oblique nozzle angle (Ψ) display

Mesh structure is of great importance to obtain accurate results in analysis. The Figure 3 and Figure 4 show a front and back half view for a nozzle connection placed at a 15-degree angle. A more refined meshing process has been applied for the paths (see Figure 6) to be examined here. The nozzle circumference and pad surface are divided into 8 areas and a reasonable

mapping mesh structure is obtained. Here, ASTM A266 Grade 2 Carbon Steel material with 190GPa Young's modulus and 0.29 Poisson's ratio was used as the nozzle material. Shell and pad material are the same which are A-516 Grade 70 Carbon steel pressure vessel plates. The value of Young's modulus is 200GPa and Poisson's ratio is 0.29. In addition, the whole model is restricted to movement in all directions by means of the saddles, which can be seen in Figure 1. Shell and nozzles are free to move in all directions.

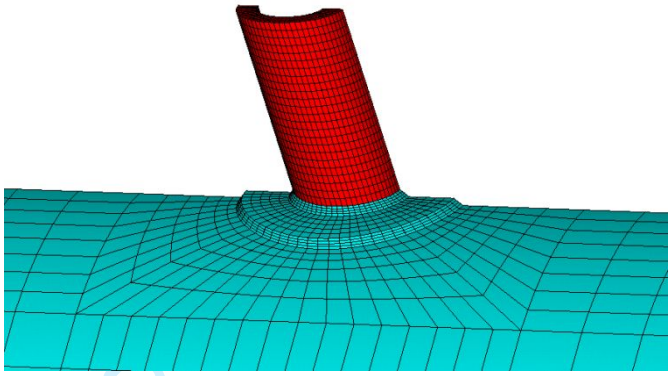

Figure 3 Front view of the half-meshed model

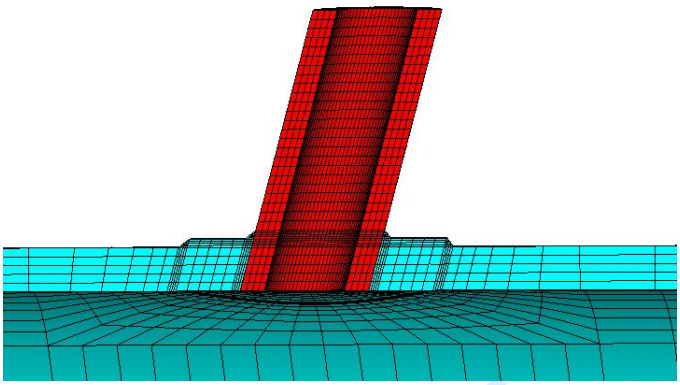

Figure 4 Back view of the half-meshed model

2.2. Validation of Finite Element Modelling

A validation study was undertaken for the finite element model to be used in this section. The calculations made by Moss et al. [24] are used in the verification study. Although the suggested calculations are not suitable for every case, certain parameters have been determined in large diameter nozzle openings cases. The applicability of this method to cases where the procedure is considered safe has been revised by ASME. The authors stated that if the information given below is exceeded, FEA should be used. In the light of this information, the FEM approach to be used in the analysis was rearranged for large diameter nozzles according to the parameters given below and membrane stresses were compared.

Parameters for calculations performed:

a. Vessel diameter > 152.4cm
b. Nozzle diameter > 101.6cm
c. Nozzle diameter > $3.4\sqrt{Dt}$ – the die-out distance
d. d/D < 0.7

Based on the parameters given above, dimensions were determined as Di=2000mm, di=1200mm, t=100mm and T=100mm. Membrane stress calculations for padded and non-padded nozzles are given in Equation 1 and Equation 2, respectively.

$$\sigma_m = P\left[\frac{\left(D_i\left(d_i + t + \sqrt{D_m T}\right) + D_i\left(T + T_e + \sqrt{d_m t}\right)\right)}{A_s}\right] \quad (1)$$

$$\sigma_m = P\left[\frac{\left(D_i\left(d_i + t + \sqrt{D_m T}\right) + D_i\left(T + T_e + \sqrt{dt}\right)\right)}{A_s}\right] \quad (2)$$

A 50% pad contribution was applied in the FE analysis performed and the results obtained with the hand calculation are compared in the Figure. Since there is a pad in the model, the membrane stress (σ_m) was calculated using Equation 1. The FEA and hand calculation results obtained are 99.1% compatible with each other as shown in the **Figure 5**.

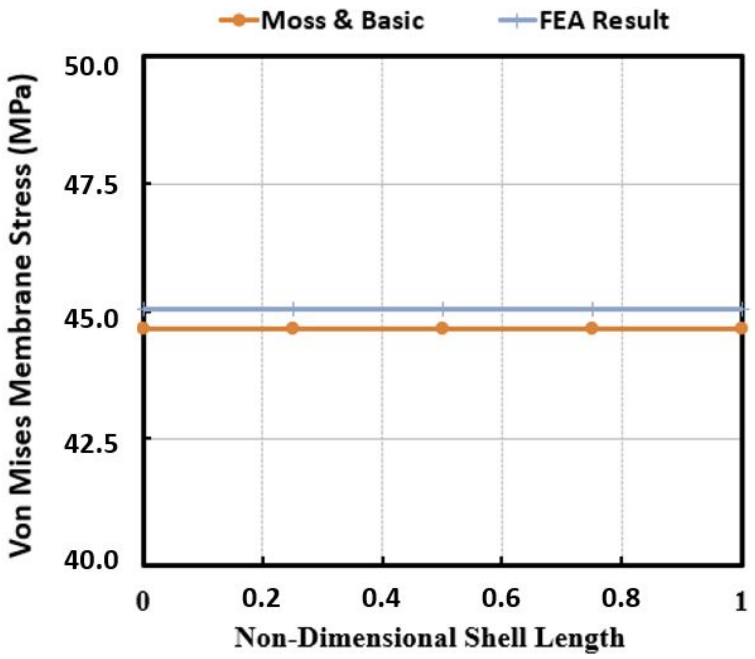

Figure 5. Comparison of the Von-Mises FEA and Moss Equation results

3. RESULTS AND DISCUSSION

3.1. Stress Linearization Analysis (SLA)

Stress linearization is a procedure in which the stress distribution along a line through the thickness in a solid is approximated with an equivalent linear stress distribution, similar to what would be the result of an analysis using shell theory. An overall stress distribution is obtained in an analysis made using the finite element method. Therefore, in order to obtain membrane and bending stresses, the total stress distribution must be linearized on the basis of the stress component. Stress linearization is the separation of stresses along a section into constant membrane and linear bending stresses. In simpler terms, a section is defined on the model that is desired to be examined. The starting and ending positions are defined with thanks to the coordinates of the nodes in the selected section. The path between this selected start and end points can be called the stress line. Now, 2-dimensional stress linearization calculations can be

performed on this defined stress line with the help of an FEA program. In addition to this method, Stress Integration Method, Structural Stress Method Based on Nodal Forces and Structural Stress Method Based on Stress Integration techniques can also be used to linearize finite element results. What all these methods have in common is that they can typically be performed with post-processing tools provided by commercial finite element analysis software.

In this section, stress distributions for some locations in oblique nozzles connections are examined. For these analysis, 6 critical paths were identified as shown in the **Figure 6**. The path number 1 represents the intersection of the nozzle with the Shell top point and shows the distribution of stress from the nozzle outer wall to the inner wall. The path number 2 represents the intersection point of the top of the pad and the nozzle. The path number 3 is from a weld top point and nozzle combination to nozzle inner wall. The path number 4 is the joining line between the shell and the nozzle and stress change from shell inner wall to outer wall is examined. The path number 5 was determined as a path between Shell and the weld origin starting point in a similar approach to path number 4. Von-Mises stress distributions is obtained in all analysis. In all cases, Membrane and Total stress values will be plotted comparatively.

It should also be noted that, stress contours obtained in finite element analyzes are available to obtain very close but different peak stresses in the maximum region according to the capabilities of the user in these software (modelling, meshing, etc.). For this reason, in order to avoid these peak stresses, a path that directly contacts the crotch corner, where the maximum stress concentration occurs, was not chosen while determining the SLA paths.

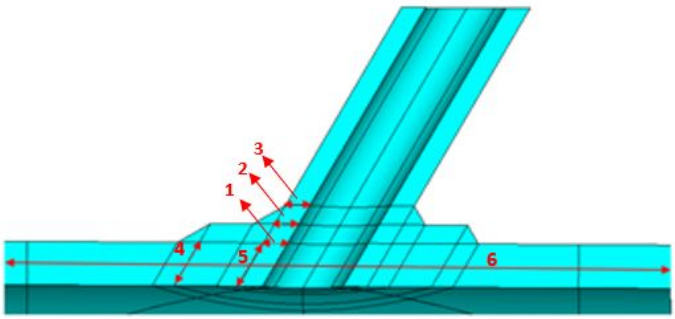

Figure 6. Determined paths to be analysed for oblique nozzle

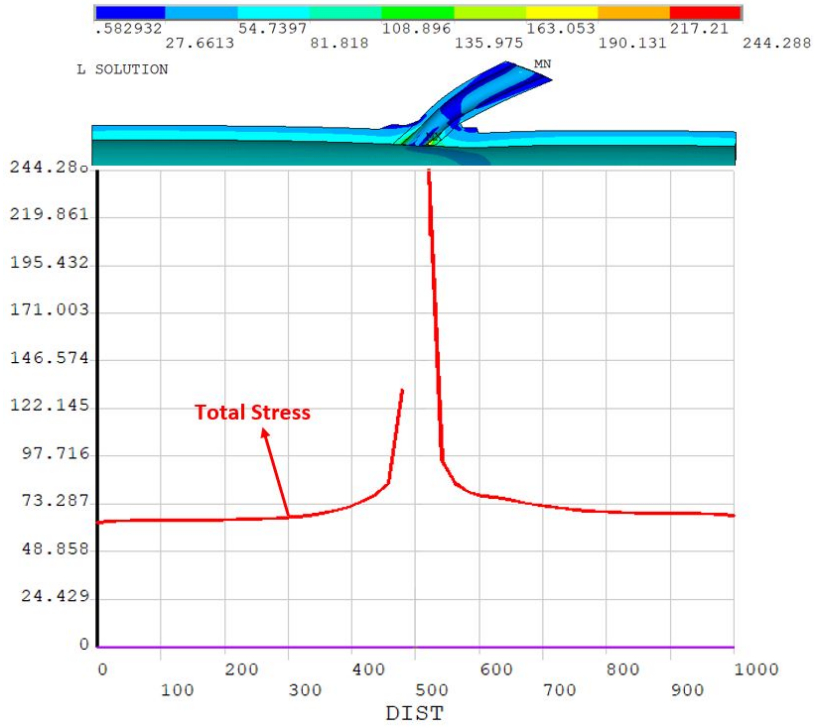

Figure 7 FEA Stress distribution and a Stress linearization representation

In addition, analysis takes place in 3 states for oblique nozzles. Firstly, the oblique nozzle angle change and then, secondly, the pad contribution effect for a specific nozzle angle is established. Finally, the influence of changing the pad diameter is investigated. In the **Figure 7**, a representative FEA solution and stress linearization graph are plotted for a pad reinforced nozzle-cylinder intersection with an oblique nozzle angle of 45 degrees.

In the following steps, the effect of pad contribution is investigated first. For this, the pad thickness is increased regularly for a low inclined oblique nozzle. Then, the effect of pad diameter on stress values is investigated. Then, the effects of changing the oblique nozzle angle on the strain linearization for a constant pad contribution is discussed.

3.2. Effect of the Oblique Nozzle Angle (Ψ)

In this section, a cylindrical pressure vessel with a single nozzle under constant 5MPa pressure is examined for stress variations for the 6 critical paths mentioned. In these analyses, di/Di = 0.083 and t/T = 0.55. There is a 50 percent pad contribution in all issues (Tp/T = 0.5). The only variable in the analysis is the nozzle angle. SLA analyses were repeated for 0 degrees (vertical nozzle), 15 degrees, 30 degrees and 45 degrees nozzle angle. The obtained Von-Mises Membrane and Total stress values are given in the figures below.

When the **Figures 8-10** were examined, the stress linearization changes along the nozzle thickness are examined in 3 different locations. These can be briefly called pad bottom (1), pad top (2) and welding top (3). In nozzle joint problems, the tension values in the opening zone are maximum. That is why, stress values tend to increase as approaches the crotch corner. When the graphics are checked out within themselves, both membrane and total stress values increase as the nozzle angle increases. In addition, the highest stress values were obtained in path number 1. However, when the nozzle angles of 0 degrees and 45 degrees are compared in membrane stress plots, the differences are approximately 14% for path number 1, 34% for path

number 2, and 45% for path number 3. Total stress values increase from the nozzle outer wall to the inner wall in all graphical output plots.

Paths 4 and 5 represent the closest and farthest shell thickness to the nozzle under the pad. The stress distribution is from the outer wall of the shell to the inner wall. The distribution of total stress values on path number 4 is very close to each other and the difference is less than 6% at the maximum point. On path number 5, the stress is maximum at the 45-degree nozzle at the initial starting point, and the difference to 0 degrees is close to 20 percent. The stress values are very close to each other at the point closest to the crotch corner and the maximum difference is less than 4%. The results are shown in the **Figures 11-12**.

Finally, stress values were obtained along top of the shell is from beginning and end point of the shell (path number 6). The reason for the gap in the graphics is the nozzle opening and opening dimension is outer diameter of the nozzle. Membrane stress as shown in the Figure is 60.3MPa and constant for a vertical nozzle with an angle of 0 degrees. On the other hand, as the nozzle angle increases, this uniformity is lost on both sides of this opening. The most important point is that the stresses are higher where the nozzle bends. Although the difference in stress values is much less than 1 percent here, it is important for stress distribution studies. In the total stress graph in **Figure 13**, while the stress distribution moves steadily along the shell, the stress reaches the peak point as it goes on the nozzle.

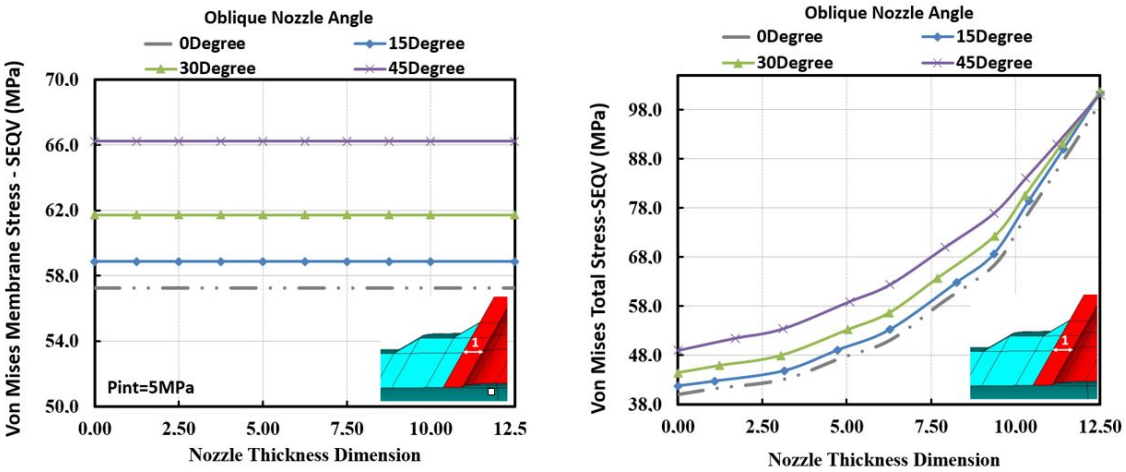

Figure 8. Von-Mises SLA results with changing nozzle angle (Path 1)

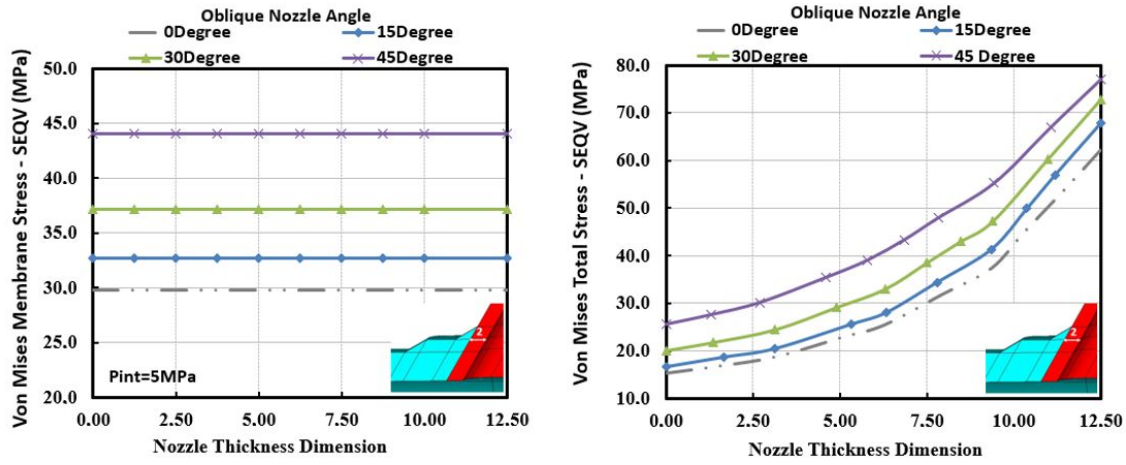

Figure 9. Von-Mises SLA results with changing nozzle angle (Path 2)

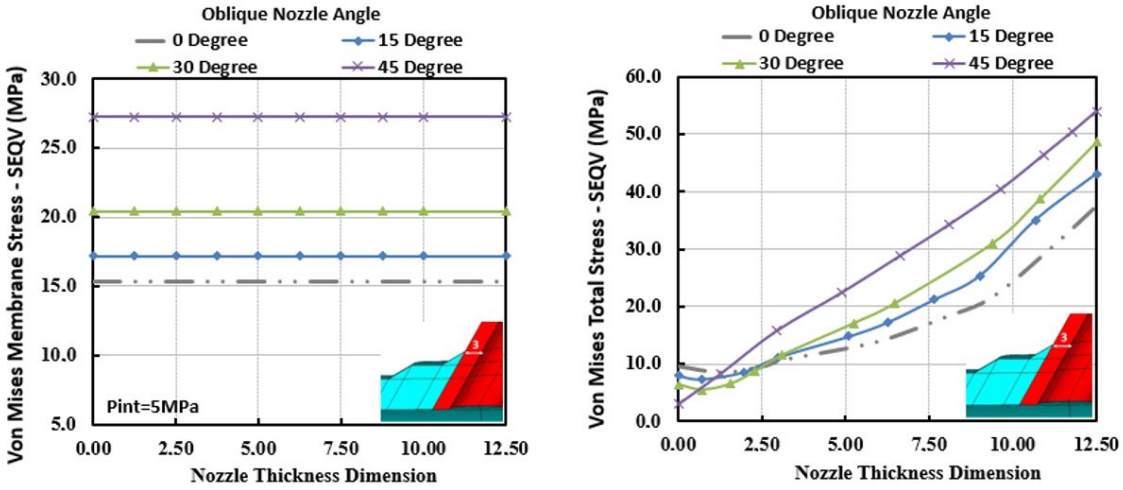

Figure 10. Von-Mises SLA results with changing nozzle angle (Path 3)

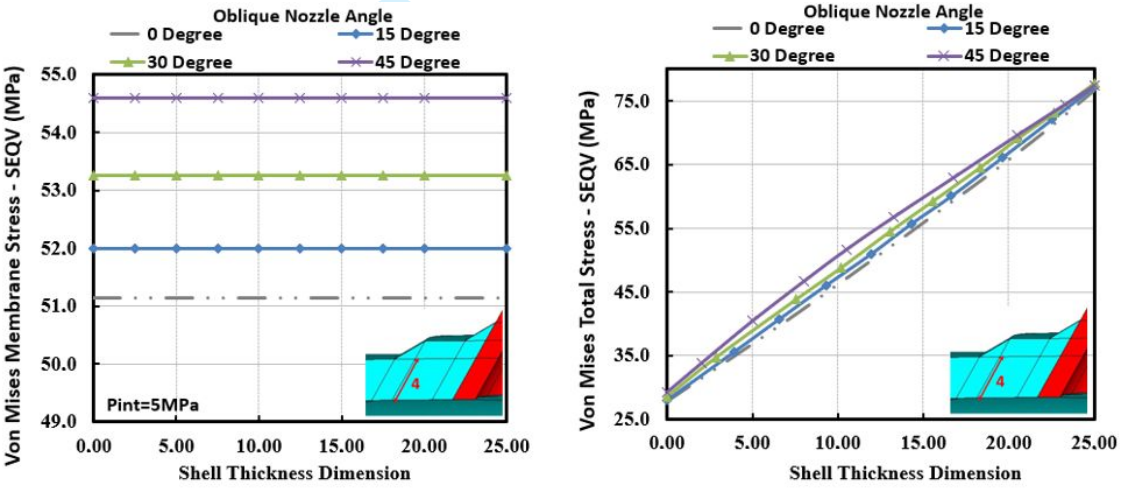

Figure 11. Von-Mises SLA results with changing nozzle angle (Path 4)

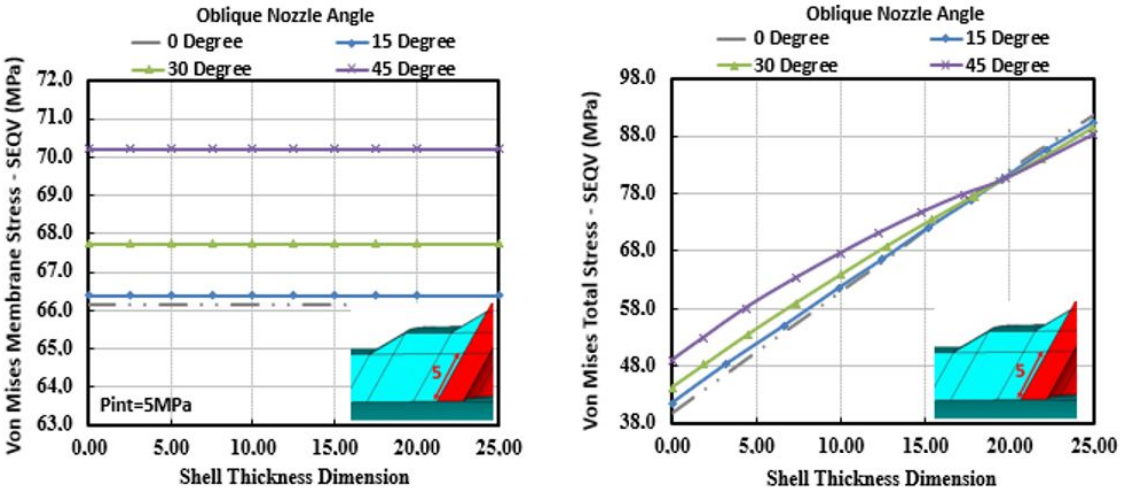

Figure 12. Von-Mises SLA results with changing nozzle angle (Path 5)

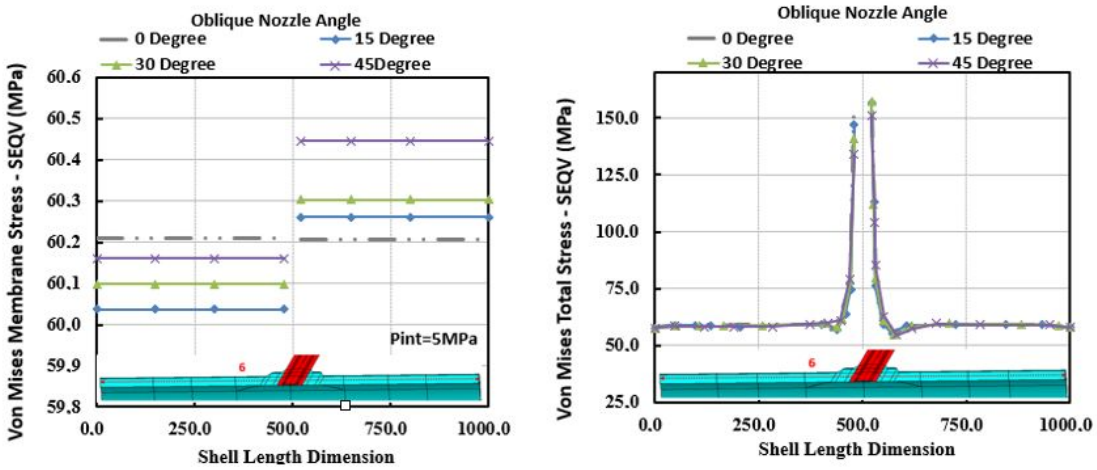

Figure 13. Von-Mises SLA results with changing nozzle angle (Path 6)

3.3. Effect of the Pad Contribution

In this section, the effect of pad contribution on stress linearization is studied. The paths to be investigated are the same as in the previous section. Similarly, an internal pressure of 5MPa was applied to the inner wall of the system. di/Di and t/T ratios are again similar the previous analyses. Furthermore, the nozzle angle is determined as 15 degrees. The analyses will be examined in 4 stages, these are 0% (no pad), 25%, 50% and 75% pad additions. (% pad contribution = Tp/T * 100)

The paths to be examined in the nozzles are selected as pad bottom (1), pad top (2) and welding top (3). Due to the absence of a pad contribution in the case of 0% contribution, paths 1 and 2 were eliminated automatically. For the connection between graphics to be consistent, 0% pad contribution status will be ignored in path number 3.

When **Figures 14-16** are examined, it can be observed that the membrane and total stress values of the nozzle decrease as the pad contribution increases. Among these 3 paths, the closest path to the maximum stress zone is the path number 1. When paths 1 and 3 are examined among themselves, membrane stress values of path number 3 are 50% less than path number 1 at the minimum point. In path number 1, the membrane stress difference between 25% additive and 50% additive is 2.7%, while the difference between 50% pad contribution and 75% pad contribution is 0.6%. These differences are greater in paths 2 and 3. The reason for this is that as the pad contribution increases, the 2 and 3 paths are located at points farther from the critical area.

When the 4th and 5th paths are examined in **Figure 17-18,** stress changes can be easily observed throughout the shell thickness. 0% pad contributions have also been examined in these graphs. As can be seen from the graphics, the pad contribution reduced the stress 6% at the minimum point.

In path number 6, the stress values on the side where the nozzle is inclined are on average 0.5% higher. As seen in the total stress graph in **Figure 19,** the stress values are almost linearly constant until the pad starts, while the tension in the area under the pad decreases and peaks at the crotch corner.

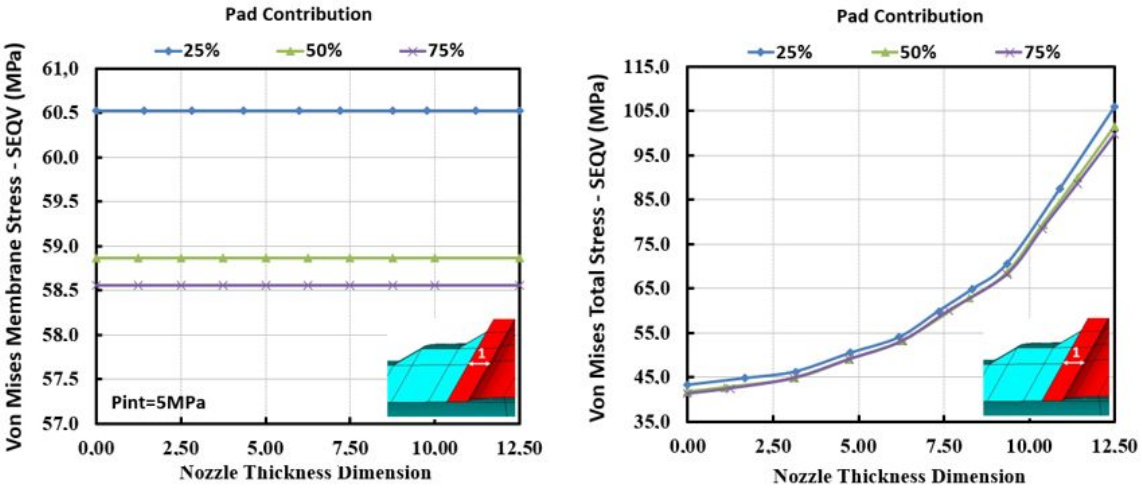

Figure 14. Von-Mises SLA results with changing pad contribution (Path 1)

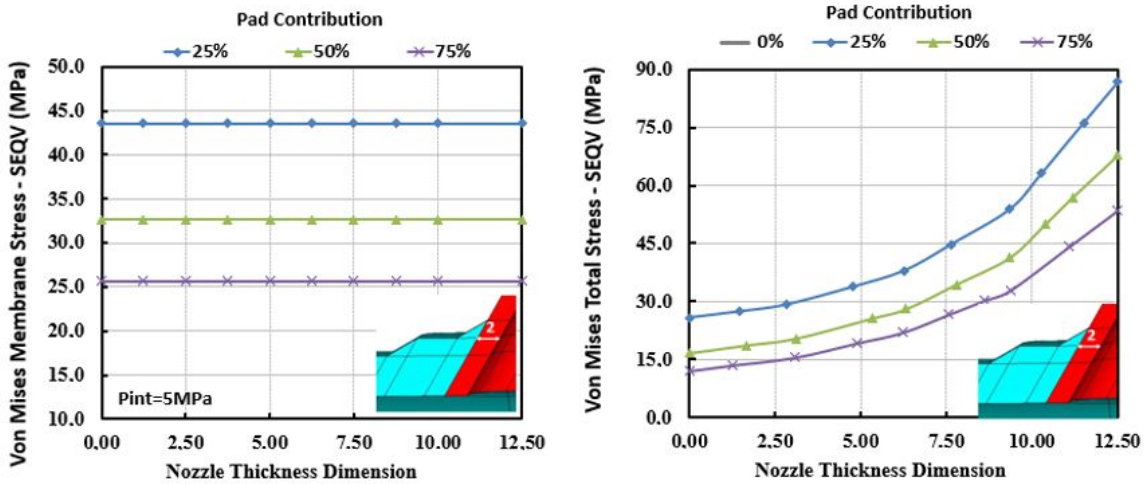

Figure 15. Von-Mises SLA results with changing pad contribution (Path 2)

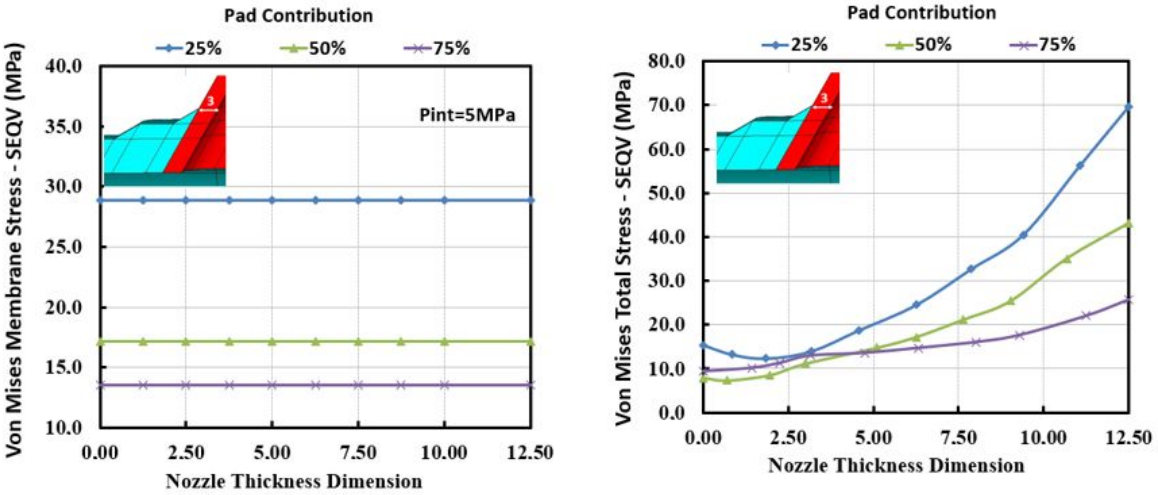

Figure 16. Von-Mises SLA results with changing pad contribution (Path 3)

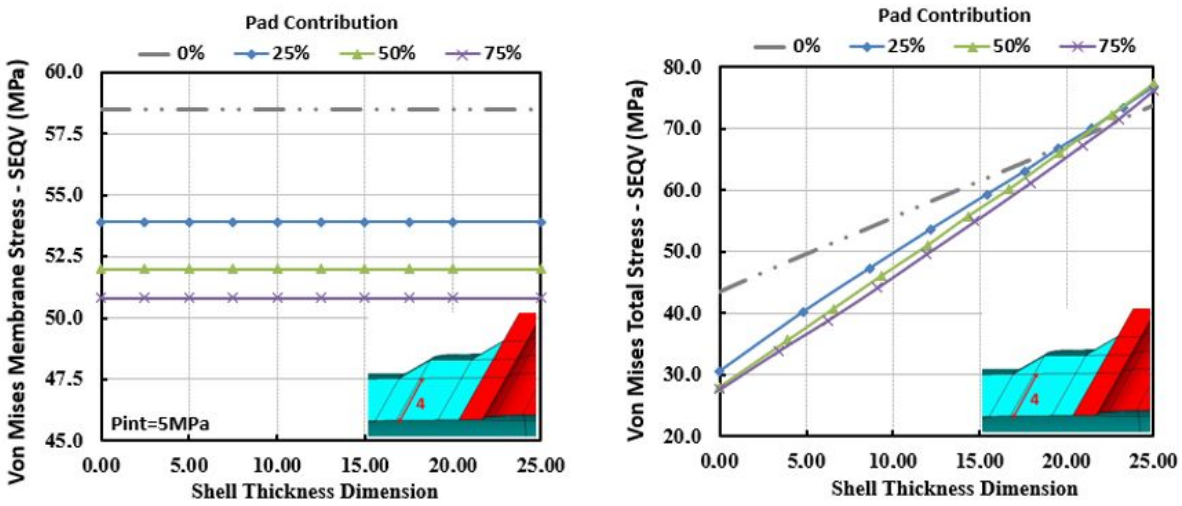

Figure 17. Von-Mises SLA results with changing pad contribution (Path 4)

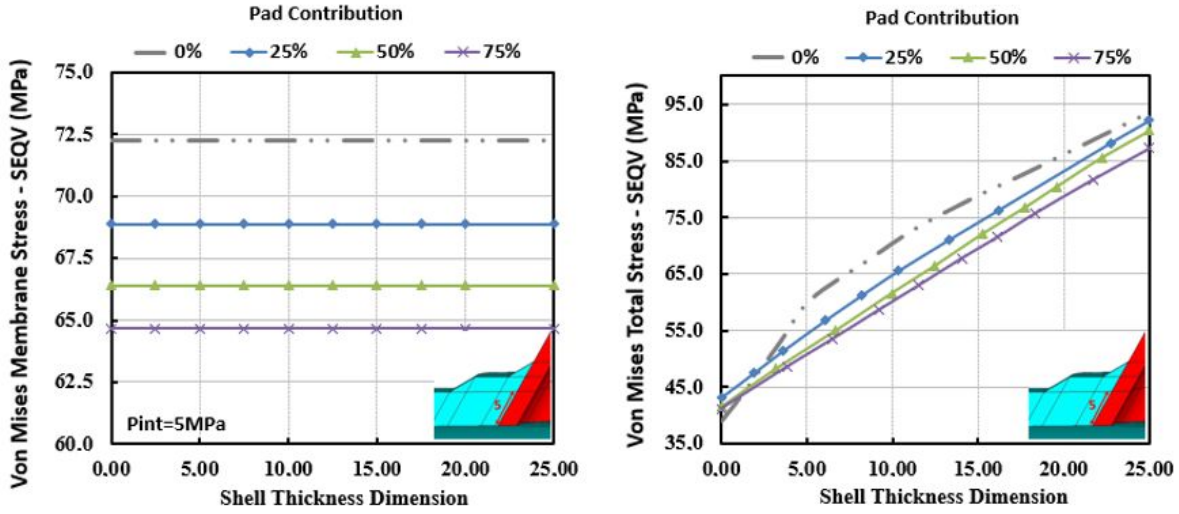

Figure 18. Von-Mises SLA results with changing pad contribution (Path 5)

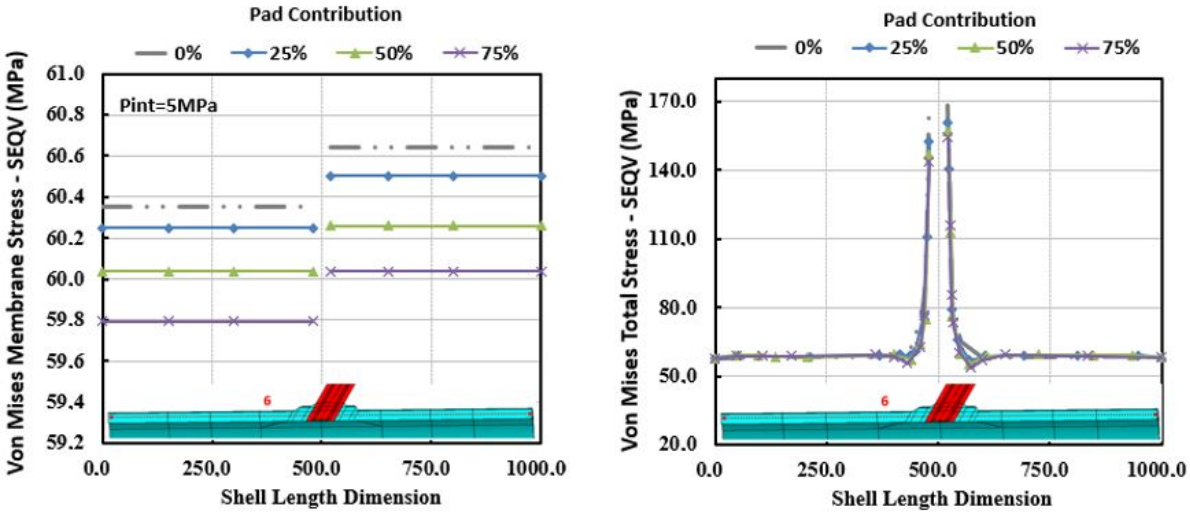

Figure 19. Von-Mises SLA results with changing pad contribution (Path 6)

3.4. Effect of the Pad Diameter Changing

In this section, the relationship between stress linearization and pad diameter magnitudes is considered. Unlike the other cases, the welding effect was ignored in the analyses. Since the pad diameter effect only is examined, the pad contribution around the nozzle should be equal in terms of stress distribution. For this reason, the nozzle angle should be 0 degrees, that is, a vertical nozzle should be used. In all cases, di/Di = 0.16 and T/t = 0.9. 50% pad additive was applied to the shell. Nozzle sizes are fixed and the only variable in each analysis is the pad diameter. This variable is shown as Dp/di in the graphs. For these analyses, 4 critical paths around the pad were determined. These are the thickness of the nozzle along the bottom of the pad, the thickness of the nozzle along the pad top, the border line of the nozzle and shell under the pad, and the shell thickness of the pad end point. These are named as paths 1, 2, 3, and 4 respectively and shown in the **Figure 20.**

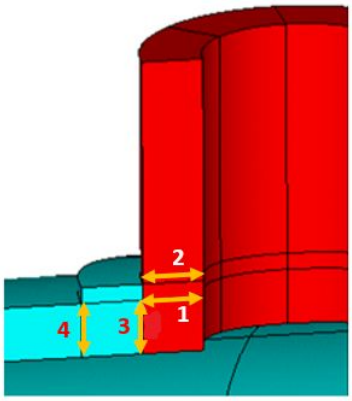

Figure 20. Determined paths to be analysed for vertical nozzle

When the paths selected on the nozzle are examined, the membrane stresses obtained in the path numbered 1 are approximately 40% more than the path number 2. In addition, as the pad diameter increased, there was a decrease in the stress values.

When the paths along the shell are examined, approximately 20% more stress occurs on the path close to the nozzle. Again, as with the nozzle, the tension values decreased as the pad diameter increased.

In both nozzle and Shell membrane stresses, the stress differences in paths numbered 1, 2 and 3 are less than 1.5%. Only on path number 4 the difference is around 6%. This happens because it moves away from the critical maximum stress zone. In total stresses, in all cases, very close to each other and approximately 1% difference were obtained. The most important point is that the stress values along the Shell show an almost linear increase, while the stress increase in the nozzle region is parabolic.

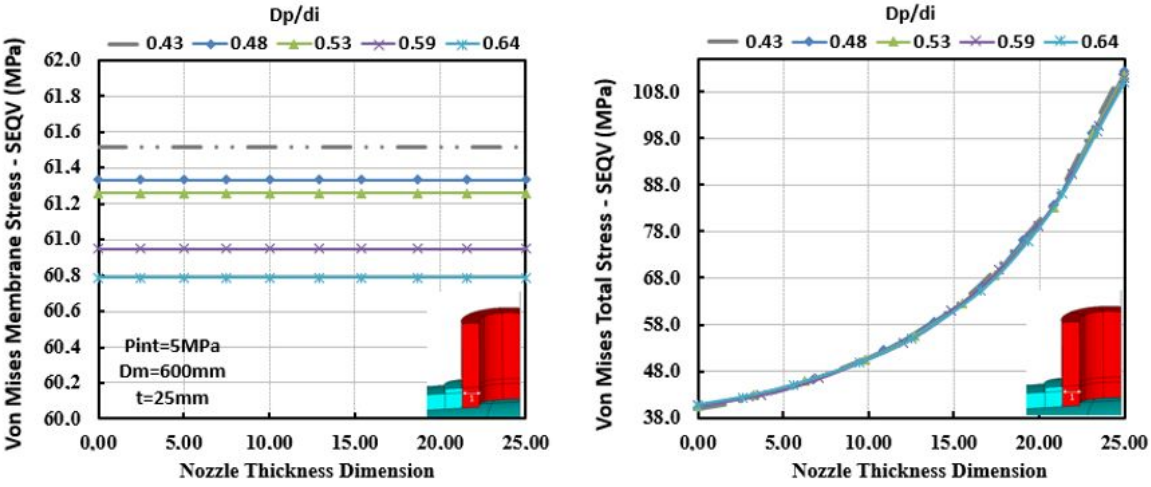

Figure 21. Von-Mises SLA results with changing pad contribution (Path 1)

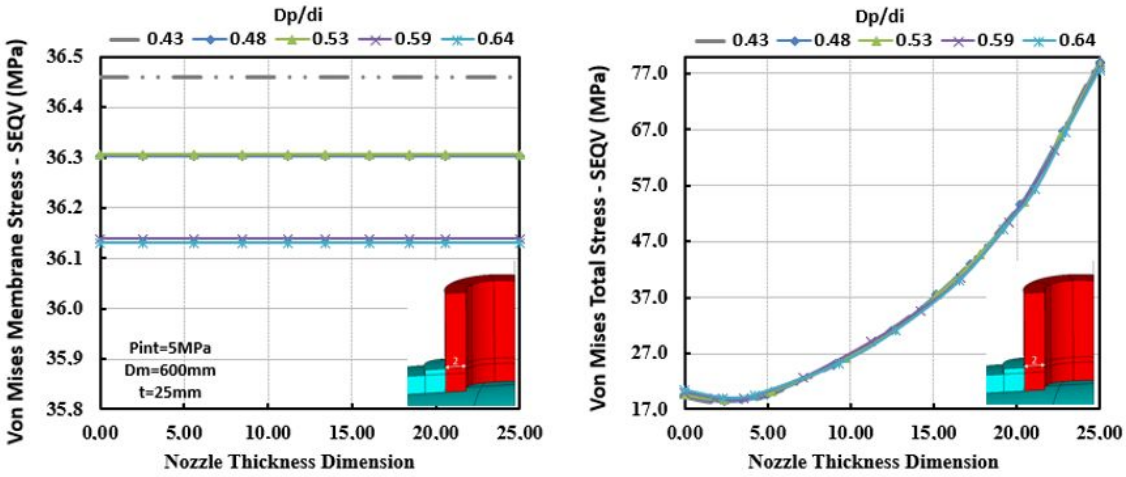

Figure 22. Von-Mises SLA results with changing pad contribution (Path 2)

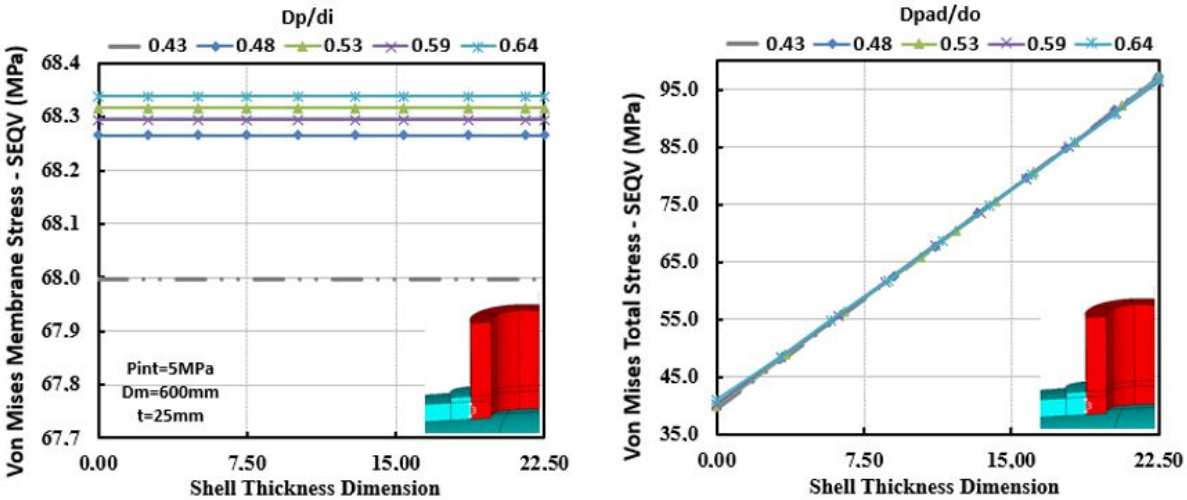

Figure 23. Von-Mises SLA results with changing pad contribution (Path 3)

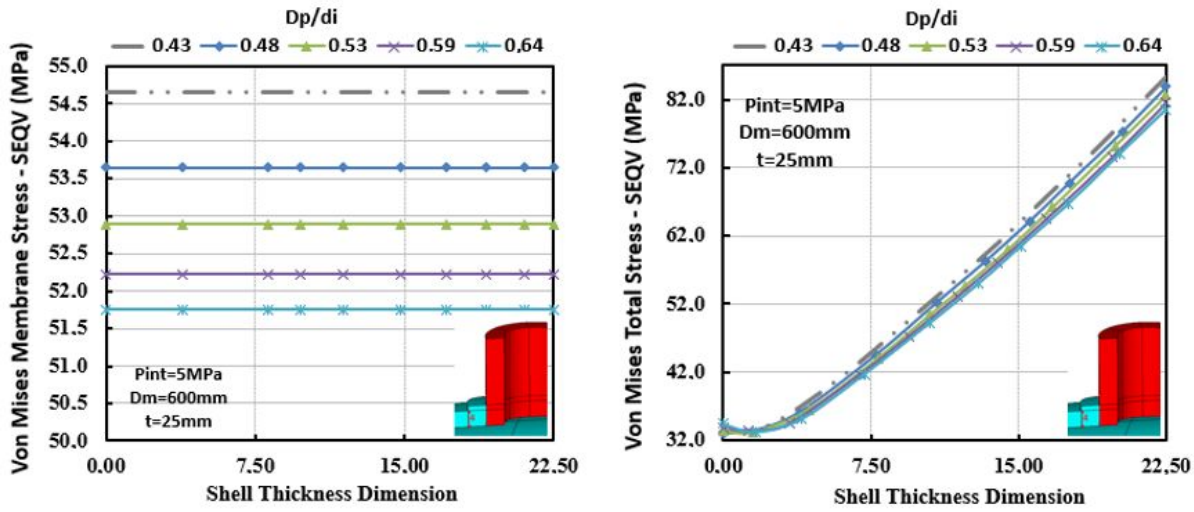

Figure 24.. Von-Mises SLA results with changing pad contribution (Path 4)

4. CONCLUSIONS

A comprehensive FEA based parameter study has been undertaken for oblique nozzles in cylindrical shells. Stress linearization is used in Pressure Vessel Design by Analysis to describe constant and linear thickness FEA (Finite Element Analysis) stress distributions and membrane and membrane plus bending stress distributions. Based on the analyses, it was carried out in 2 stages. These can be summarized as nozzle angle change and pad reinforcement effect. As a result of the calculations, it was deemed appropriate to keep the change in the nozzle angle between 0 and 45 degrees. When the nozzle thickness and the paths along the shell are examined, an increase in the stress values is observed as the crotch approaches the corner. The most important point observed here is that although the stress distribution is equal at both junctions for a 0-degree vertical nozzle, the stress distribution changes as the nozzle angle changes. This means the stresses are higher where the nozzle bends. Although the difference in stress values is much less than 1 percent here, it is important for stress distribution studies. In the total stress graph, while the stress distribution moves steadily along the shell, the stress reaches the peak point as it goes on the nozzle. The pad contribution was examined considering both the pad diameter and the pad thickness.

In summary, as a result of this study, a comprehensive stress linearization study was performed for a nozzle-cylinder combination subjected to internal pressure only. In the study, the stress distribution at the critical points determined on the nozzle and shell was investigated. According to the results, the stress is maximum in the selected paths close to the opening zone in both the shell and the nozzle. Also, the increase in pad contribution significantly reduced the stresses obtained on the same roads. On the other hand, since the stress distribution on both sides of the inclination is not equal in inclined nozzles, the differences in stress magnitudes can be easily determined by this method. In conclusion, this study offers researchers an alternative stress analysis for critical locations in the intersection area in the design and analysis of cylinder nozzle connections.

Despite all this, this study is only an answer to internal pressure problems in cylindrical vessels. This work can be extended in future studies to problems such as spherical vessels, multiple nozzle combinations, external loading conditions.

ACKNOWLEDGEMENTS

The work of M. Bozkurt was supported by the Republic of Turkey Ministry of National Education under Grant MoNE-1416/YLSY.

REFERENCES

[1] Wichman, K.R., Hopper, A.G. and Mershon, J.L. "Local Stresses in Spherical and Cylindrical Shells Due to External Loadings." *Welding Research Council Bulletin No. 107*. New York (2002)

[2] Wichman, K.R., Hopper, A.G. and Mershon, J.L. "Precision Equations and Enhanced Diagrams for Local Stresses in Spherical and Cylindrical Shells Due to External Loadings for Implementation of WRC Bulletin 107" *Welding Research Council Bulletin No. 537*. (2013)

[3] Mukhtar, F. M., & Al-Gahtani, H. J. (2017). Design-focused stress analysis of cylindrical pressure vessels intersected by small-diameter nozzles. *Journal of Pressure Vessel Technology*, *139*(2).

[4] Mukhtar, F. M., & Al-Gahtani, H. J. (2016). Finite Element Analysis and Development of Design Charts for Cylindrical Vessel–Nozzle Junctures Under Internal Pressure. *Arabian Journal for Science and Engineering*, *41*(10), 4195-4206.

[5] Al-Gahtani, H. J., & Mukhtar, F. M. (2016). Simplified Formulation of Stress Concentration Factors for Spherical Pressure Vessel–Cylindrical Nozzle Juncture. *Journal of Pressure Vessel Technology*, *138*(3).

[6] Mukhtar, F. M., & Al-Gahtani, H. J. (2019). Comprehensive Evaluation of SCF for Spherical Pressure Vessels Intersected by Radial Cylindrical Nozzles. *International Journal of Steel Structures*, *19*(6), 1911-1929.

[7] Bozkurt, M., Nash, D., & Uzzaman, A. (2019, July). Investigation of the stresses and interaction effects of nozzle-cylinder intersections when subject to multiple external loads. In Pressure Vessels and Piping Conference (Vol. 58943, p. V003T03A028). American Society of Mechanical Engineers.

[8] Bozkurt, M., Nash, D., & Uzzaman, A. (2021). A comparison of stress analysis and limit analysis approaches for single and multiple nozzle combinations in cylindrical pressure vessels. *International Journal of Pressure Vessels and Piping*, 194, 104563.

[9] Bozkurt, M. (2022). Towards a unified design-by-analysis solution to pressure vessel nozzle-shell junctions under combined loading.

[10] Muhammad Raza Cheema, Niyamatullah Ataullah Patel, Aftab Alam, 2019, Analysis of Pad Reinforced Openings in Pressure Vessels*, International Journal of Engineering Research & Technology (IJERT)* Volume 08, Issue 08 (August 2019)

[11] Mershon, J.L., Mokhtarian, K., Ranjan, G.V. and Rodabaugh, E.C. "Local Stresses in Cylindrical Shells Due to External Loadings on Nozzles-Supplement to WRC Bulletin No. 107 (Revision I)" *Welding Research Council Bulletin No. 297*. (1984)

[12] Avinash R. Kharat, S.J. Kadam, S.G. Bhosale, 2013, Study of different type reinforcement in cylindrical pressure vessel, *International Journal of Engineering Research & Technology (IJERT)* Volume 02, Issue 10 (October 2013)

[13] Xue, L., Widera, G. E. O., & Sang, Z. F. (2003). Influence of pad reinforcement on the limit and burst pressures of a cylinder-cylinder intersection. *J. Pressure Vessel Technol.*, 125(2), 182-187.

[14] Fang, J., Tang, Q. H., & Sang, Z. F. (2009). A comparative study of usefulness for pad reinforcement in cylindrical vessels under external load on nozzle. *International journal of pressure vessels and piping*, 86(4), 273-279.

[15] Chao, Y. J., Wu, B. C., & Sutton, M. A. (1986). Radial flexibility of welded-pad reinforced nozzles in ellipsoidal pressure vessel heads. *International journal of pressure vessels and piping*, 24(3), 189-207.

[16] Nash, D. H., & Hitchen, J. (2009, September). Effects of local reinforcement on nozzles in dished ends. In 12th International Conference on Pressure Vessel Technology, ICPVT-12 (pp. 1-13).

[17] Skopinsky, V. N., & Smetankin, A. B. (2003). Parametric study of reinforcement of pressure vessel head with offset nozzle. *International journal of pressure vessels and piping*, 80(5), 333-343.

[18] Petrovic, A. L., Balac, M. M., Jovovic, A., & Dedic, A. (2012). Oblique nozzle loaded by the torque moment–stress state in the cylindrical shells on the pressure vessel. *Proceedings of the Institution of Mechanical Engineers, Part C: Journal of Mechanical Engineering Science*, 226(3), 567-575.

[19] Weiß, E., Rauth, M., & Rudolph, J. (1998). Fatigue behaviour of oblique nozzles on cylindrical shells submitted to internal pressure and axial forces. *International journal of pressure vessels and piping*, 75(6), 473-481.

[20] Dilip M. Patel, Dr. Bimlesh Kumar, 2013, Limit Load Estimation of Cylindrical Vessel with Oblique Nozzle, *International Journal Of Engineering Research & Technology (IJERT)* Volume 02, Issue 11 (November 2013)

[21] Robinson, M., Kirk, A., & Gill, S. S. (1971). An experimental investigation into the plastic behaviour of oblique flush nozzles in spherical pressure vessels. *International Journal of Mechanical Sciences*, 13(1), 41-46.

[22] ANSYS v19, Finite Element Code, ANSYS Inc, 2019

[23] PD 5500:2021, Specification for unfired fusion welded pressure vessels

[24] Moss, D. R., & Basic, M. (2013). 6-Special Design. Pressure Vessel Design Manual (Fourth Edition) (p. 393-434).